

Numerical Analysis of Fluid Flow and Heat Transfer Characteristics of Ventilated Disc Brake Rotor Using CFD

¹A. Rajesh, ²K. Vedhagiri, ³L.Sivaprasanth, ⁴R. Vengatesh
^{1,2,3,4}Department of Mechanical Engineering, Sri Ramanujar engineering College
Chennai-127

Abstract: - Ventilated brake discs are used in high speed automobiles. The brake disc is an important component in the braking system which is expected to withstand and dissipate the heat generated during the braking event. In the present work, an attempt is made to study the effect of vane-shape rotor on the flow-field and heat transfer characteristics for different configurations of vanes for different running speeds using commercial CFD tool. Two types of rotor configurations circular pillared (CP) and diamond pillared radial vane (DP) were considered for the numerical analysis. A rotor segment of 20° was considered for the numerical analysis due to rotational symmetry. The pre processing is carried out with the help of ICEMCFD and analysis is carried out using ANSYS CFX 12.1. The governing equations namely conservation of mass, momentum and energy are solved for the analysis. The predicted results are validated by the experimental studies available in the literature. The mass flow rate, heat dissipated by the circular pillared vanes are compared with the diamond pillared vanes. The heat dissipation rate through the diamond pillared vanes is more uniform at higher speeds.

Keywords: - CFD, Disc brake, Rotational Symmetry, Vane Shape, DP.

I. INTRODUCTION

Braking system is one of the important safety components of an automobile [2]. It is mainly used to decelerate vehicles from an initial speed to a given speed. Friction based braking systems are the common device to convert kinetic energy into thermal energy through friction between the brake pads and the rotor faces. Excessive thermal loading can result in surface cracking, judder and high wear of the rubbing surfaces. High temperatures can also lead to overheating of brake fluid, seals and other components. Based on their design configurations, friction brakes can be grouped into disc and drum brakes. The drum brakes use brake shoes that are pressed in a radial direction against a brake drum. The disc brakes use pads that are pressed axially against a rotor or disc. Under extreme conditions, such as descending a steep hill with a heavy load, or repeated high-speed decelerations, drum brakes would often fade and lose effectiveness. Compared with their counterpart, disc brakes would operate with less fade under the same conditions. Advantages of disc brakes over drum brakes have led to their universal use on passenger- car and light-truck front axles, many rear axles, and medium-weight trucks on both axles. Thus, how to select better geometrical design variables and improve thermal performance of automotive brake rotors is a task that the vehicle designers and researchers are often confronted.

The air flow through the passage of vane rotors is complex due to the turbulence induced across the vane passages [3]. With an analytical method, it is difficult to determine the effects of geometries of rotors on thermal performance of disc brakes. In the present work, two types of disc brake rotors, Circular Pillared (CP) and diamond pillared vane (DP) are analyzed for the effect of vane -shape rotor on the flow-field and heat transfer characteristics for different configurations of vanes for different running speeds using commercial CFD tool.

II. COMPUTATIONAL MODELING AND SIMULATION

A. Geometrical Modeling

Fig. 1 Shows the dimensions of the disc brake rotor used for CFD analysis [1]. A 20° section of the ventilated brake rotor is created in CATIA pre-processor as shown in figure1. Only 20° sector of the ventilated vane rotor is considered due to periodic nature of the rotor brake discs. The dimensions of circular pillar vane are similar to the model in literature [1]. Fig 2 and 3 shows the circular pillared and modified taper radial vane rotors created in CATIA modeling tool.

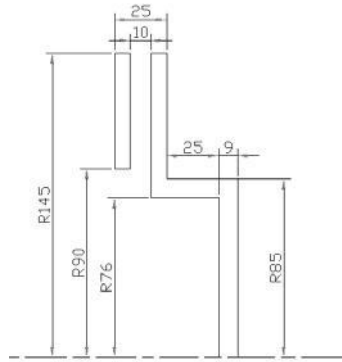


Figure 1. Disc Brake Rotor

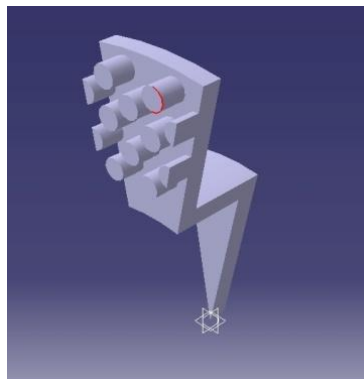


Figure 2. 20° Sector of Circular Pillared Vane created in CATIA

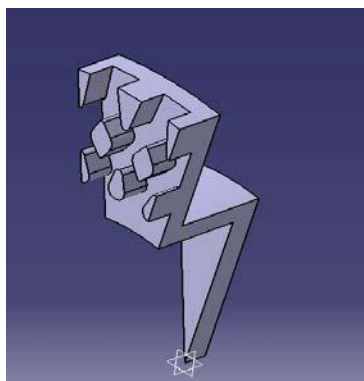


Figure 3. 20° Sector of Diamond Pillared Vane created in CATIA

B. Grid Generation

The 3-D model is then discretized in ICEM CFD pre-processing tool. In order to capture both the thermal and velocity boundary layers the entire model is discretized using hexahedral mesh elements which are more accurate and involve less computation effort. Fine control on the hexahedral mesh near the wall surface allows capturing the boundary layer gradient accurately. The entire geometry is divided into three fluid domains FLUID_STATOR ,FLUID_ROTOR_OUTER and FLUID_ROTOR_INNER. The discretised model is checked to have a minimum angle of 27° and min determinant quality of 65 %. Once the meshes are checked for free of errors and minimum required quality it is exported to ANSYS CFX pre-processor. Fig 4 and 5 shows the fluid mesh around Circular pillar and Diamond pillared vanes respectively.

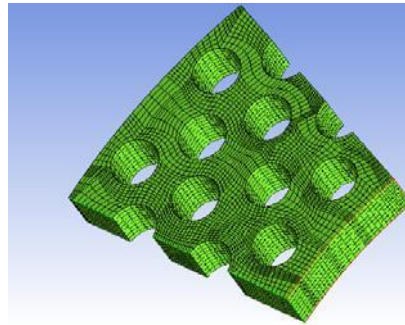


Figure 4. Hexahedral Fluid mesh around Circular Pillared vanes

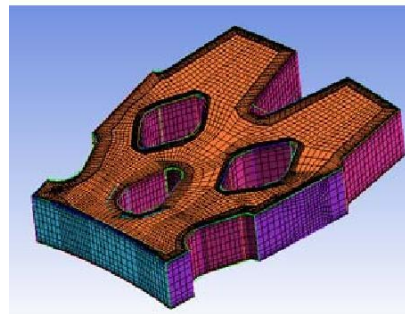


Figure 5. Hexahedral Fluid mesh around Diamond pillared Vane

C. Governing equations

The 3-dimensional flow through rotor vanes was simulated by solving the appropriate governing equations viz. conservation of mass, momentum and energy using ANSYS CFX 12.1 code. Turbulence is taken care by Shear Stress Transport (SST) $k-\omega$ model of closure which has a blending function that supports Standard $k-\omega$ near the wall and Standard $k-\epsilon$ elsewhere.

$$\text{Conservation of mass: } \nabla \cdot (\rho \vec{V}) = 0$$

$$\text{x-momentum: } \nabla \cdot (\rho u \vec{V}) = -\frac{\partial p}{\partial x} + \frac{\partial \tau_{xx}}{\partial x} + \frac{\partial \tau_{yx}}{\partial y} + \frac{\partial \tau_{zx}}{\partial z}$$

$$\text{y-momentum: } \nabla \cdot (\rho u \vec{V}) = -\frac{\partial p}{\partial y} + \frac{\partial \tau_{xy}}{\partial x} + \frac{\partial \tau_{yy}}{\partial y} + \frac{\partial \tau_{zy}}{\partial z} + \rho g$$

$$\text{z-momentum: } \nabla \cdot (\rho u \vec{V}) = -\frac{\partial p}{\partial z} + \frac{\partial \tau_{xz}}{\partial x} + \frac{\partial \tau_{yz}}{\partial y} + \frac{\partial \tau_{zz}}{\partial z}$$

$$\text{Energy: } \nabla \cdot (\rho e \vec{V}) = -p \nabla \cdot \vec{V} + \nabla \cdot (K \nabla T) + q + \phi$$

SST k equation

$$\frac{\partial k}{\partial t} + U_j \frac{\partial k}{\partial x_j} = P_k - \beta^* k \omega + \frac{\partial}{\partial x_j} \left[(\nu + \sigma_k \nu_T) \frac{\partial k}{\partial x_j} \right]$$

SST ω equation

$$\frac{\partial \omega}{\partial t} + U_j \frac{\partial \omega}{\partial x_j} = \alpha S^2 - \beta \omega^2 + \frac{\partial}{\partial x_j} \left[(\nu + \sigma_\omega \nu_T) \frac{\partial \omega}{\partial x_j} \right] +$$

$$2(1 - F_1) \sigma_{\omega 2} \frac{1}{\omega} \frac{\partial k}{\partial x_i} \frac{\partial \omega}{\partial x_i}$$

D. Boundary Condition Setup

Numerical flow analysis through ventilated brake rotors consists of three fluid domains namely FLUID_STATOR, FLUID_ROTOR_OUTER and FLUID_ROTOR_INNER. Solid domain for rotor vanes are not created separately as isothermal wall boundary conditions are specified as 900 K for speeds 1000 and 1500 rpm, 1500 K for speed 2000 rpm due to increase in heat on the rotors[6]. The flow through the ventilated brake rotors are quite complex as it involves both rotating and stationary domains. The fluid region between the rotating and stationary domains are connected by FROZEN_ROTOR interface. Turbulence is taken care by SST $k-\omega$ model of closure. The rotational periodic nature of the disc brake rotor has enabled the consideration of only a segment of it rather than complete rotor for the analysis. As each of the rotors investigated have 36 passages, a 20° segment of the rotor is modeled, large enough to avoid the effect of boundary layer [1][5]. Periodic boundaries are applied to either side of the segment to represent the entire rotor [6]. The rotors are treated as spinning in an infinite environment by a rotating frame of reference and the application of an open boundary condition to the extent of the domain. The stator domain was considered three times the rotor diameter. The flow is assumed to be steady and incompressible ideal gas. Ambient temperature and pressure are assumed as 298 K and 101325 Pa respectively. The walls were assumed to have smooth surface. For the analysis, moving frame of reference is considered, and buoyancy and radiation effects are neglected. Number of nodes used is around 4,50,0000. Fig.6 shows the entire fluid domain consisting of fluid stator and fluid rotor for circular pillared rotor vanes created in ANSYS CFX 12.1 pre processor tool. █

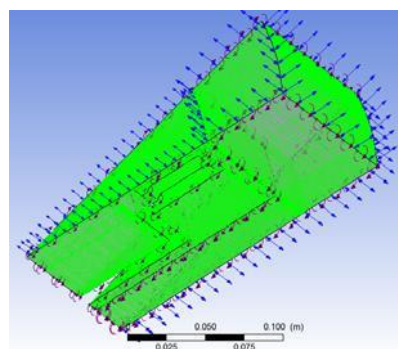


Figure 6. Fluid domain of CP Vanes created in ANSYS CFX 12.1

III. VALIDATION

The predicted mass flow rate results of circular pillared vane are compared with the results available in the literature [1]. The mass flow rate for CP obtained numerically is shown in Fig.7. A good agreement between the numerical and experimental data is obtained. The maximum deviation in mass flow rate is less than 5%. Table 1. shows the comparison of mass flow rate between numerical and literature[1] results.

Table 1. Mass flow rate of Centre Pillared Vanes

Speed (rpm)	Numerical results Mass flow rate (g/s)	Literature[1] results Mass flow rate (g/s)	Error %
1000	0.98	1.00	-1.8
1500	1.37	1.35	3.1
2000	1.66	1.71	-4.1
2500	1.95	1.90	3.8

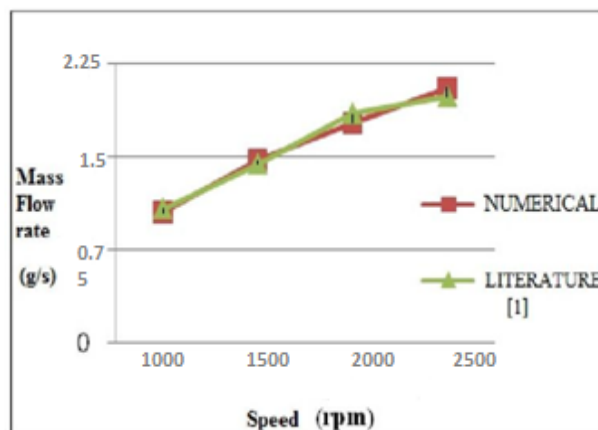


Figure 7. Mass flow rate of Centre Pillared Vanes

IV. RESULTS AND DISCUSSION

A. Mass flow rate of DP

Table 2: Shows the predicted mass flow rate of DP at different speeds. As the speed increases, the mass flow rate also increases. The increase in mass flow rate with rotational speed is higher for DP compared to CP vanes. The uniform distribution of air mass flow around the rotor vanes is essential for uniform temperature drop around the vanes. Fig 8. Shows the comparison of mass flow rate between CP and DP and it is found that the mass flow rate is around 70% more than CP for the same rotational speed.

Table 2. Mass flow rate for DP

Speed rpm	Predicted mass flow rate (g/s)
1000	2.32
1500	3.64
2000	3.92

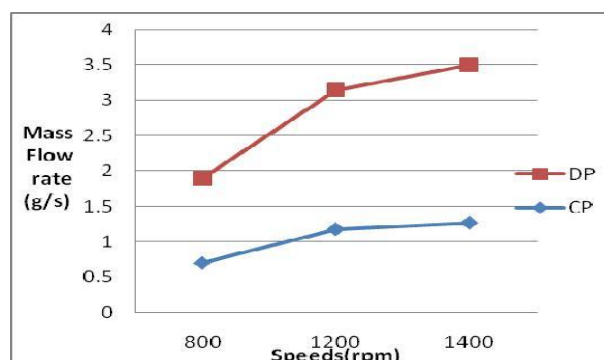


Figure 8. comparison of mass flow rate for CP and DP

B. Heat dissipation of isothermal rotors

The heat dissipation comparison for CP and DP is shown in table 3. The heat dissipated from diamond pillared vane is around 24% higher than that of circular pillared. It is found that the increased mass flow in DP has resulted in increase in heat dissipation characteristics compared to that of CP.

Table 3. Heat dissipation for CP and DP

Speed rpm	Heat dissipated(W)		% rise in heat dissipation for DP compared to CP
	CP	DP	
1000	253.68	334.67	59.64
1500	327.7	394.14	36.36
2000	519.9	631.56	36.00

C. Velocity comparison of isothermal rotors

A contour of velocity in the stationary domain and pressure in the mid plane of the rotor vanes is plotted against rpm for the rotor configurations. Fig 9 and 10. Shows the velocity distribution on mid-plane for CP and DP at speeds 1000, 1500 & 2000 rpm. In both CP and DP, the average velocity in the mid plane is increasing with increase in rotational speed. It was found that the velocity magnitude increases from zero near the hub to the maximum near the tip of the vanes for both CP and DP vanes. The velocity distribution in CP is uniform around the vanes. The velocity distribution in DP is still uniform around the vanes but can accommodate a greater mass flow due to less hindrances. The velocity distribution achieves more uniformity as the speed increases. Since a greater mass flow is passing through DP, this will induce more uniform cooling and lesser temperatures around the vanes.

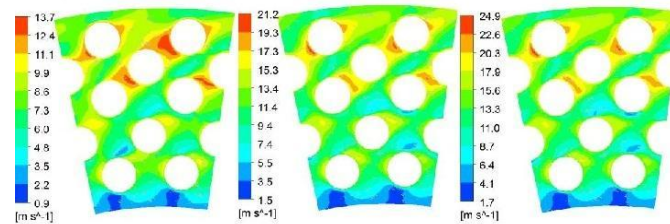


Figure 9. Velocity distribution for CP at 1000, 1500 & 2000 rpm

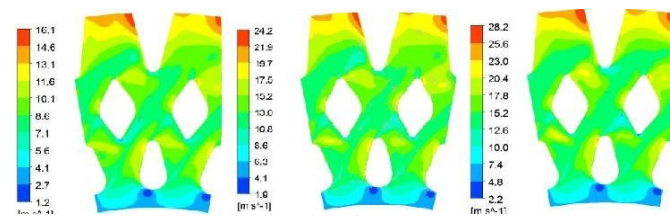


Figure 10. Velocity distribution for DP at 1000, 1500 & 2000 rpm

D. Pressure comparison of Isothermal rotors

Table 4: Shows the average pressure drop for different speeds. The average pressure drop varies at a higher rate in DP compared to CP.

Table 4. Average pressure drop for CP and DP

Speed rpm	Average pressure drop(Pa)	
	CP	DP
1000	-1.6012	-13.25
1500	-2.97166	-28.05
2000	-3.8501	-38.96

Fig 11 and 12. Shows the pressure distribution on mid plane for CP and DP at speeds of 1000, 1500 & 2000 rpm respectively. The pressure drop increases with increase in rotational speed of the rotor vanes for both DP and CP vanes. The pressure variation is almost uniform around the vanes for CP. The fluid pressure in between the rotor vanes increases slightly from minimum to maximum from hub to the tip region of DP vanes. The fluid pressure around the CP vanes is almost uniform as shown in Fig. 11. This uniform pressure distribution of CP helps in uniform thermal cooling of rotor vanes. The pressure distribution becomes uniform as speed increases. This makes more even mass flow around the vanes in DP.

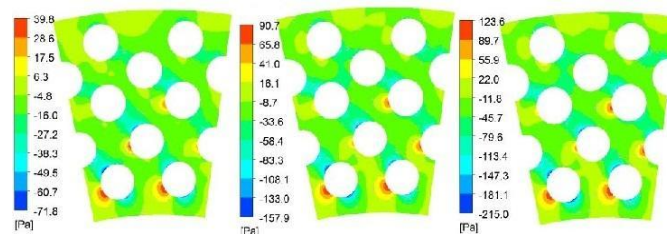


Figure 11. Pressure distribution for CP at 1000, 1500 & 2000 rpm

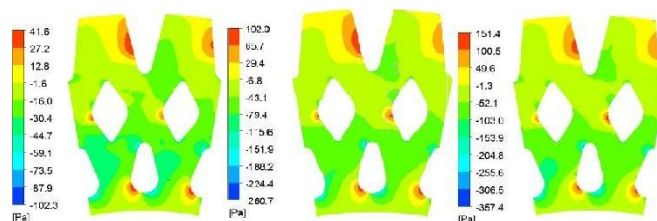


Figure 12. Pressure distribution for DP at 1000, 1500 & 2000 rpm

V. CONCLUSION

In this present work, heat transfer characteristics of Circular pillared and Diamond pillared vane are analyzed. The following conclusions are drawn.

1. Mass flow rate is considerably higher in Diamond pillared vane compared to Centre Pillared rotor vanes.
2. Heat dissipation in Diamond pillared vane is around 20% higher as that of Circular Pillared vanes.
3. Circular pillared rotor vanes have more uniform pressure and velocity distribution which results in more uniform temperature drop around the vanes.
4. The modification of circular pillared vanes to diamond pillared has resulted in more mass flow rate and better heat transfer characteristics.
5. The diamond pillared vanes are observed to have uniform pressure and velocity distribution at higher speeds. This will ensure uniform and lesser temperatures around the vanes. Due to these advantages,

diamond pillared vanes can be preferred for high speed vehicles.

REFERENCES

- [1]. S. Manohar Reddy, J. M. Mallikarjuna and V. Ganesan, Flow and Heat Transfer Analysis of a Ventilated Disc Brake Rotor Using CFD, *journal of SAE*, 2008 .
- [2]. Zhongzhe Chi, Thermal Performance Analysis and Geometrical Optimization of Automotive Brake Rotors, *University of Ontario Institute of Technology*, 2008
- [3]. Warren Chan, Analysis of Heat Dissipation in Mechanical Braking Systems, Department of Mechanical and Aerospace Engineering ,*University of California* .
- [4]. Amol A. Apte and H. Ravi, FE Prediction of Thermal Performance and Stresses in a Disc Brake System, , *journal of SAE* ,2008.
- [5]. Anders Jerhamre and Christer Bergstrom, Numerical study of brake disc cooling accounting for both aerodynamic drag force and cooling efficiency, *journal of SAE* ,2001.
- [6]. Limpert R, The thermal performance of automotive disc brakes, *journal of SAE*, 1975.
- [7]. Parish D, D. G. MacManus, Aerodynamic investigations of ventilated brake discs., *journal of Automobile Engineering*, 2005.
- [8]. Prasad Ajay K, Particle image velocimetry, *journal Of Current Science*, 2000.
- [9]. Sakamoto H, Heat convection and design of brake discs, , *journal of Rail and Rapid Transit*, 2004.
- [10]. Voller G. P, M. Tirovic, R. Morris and P. Gibbens Analysis of automotive disc brake cooling characteristics, *journal of Automobile Engineering* , 2003.
- [11]. Rajagopal, T. K.: Numerical Investigation of Fluid Flow and Heat Transfer, THERMAL SCIENCE: Year 2014, Vol. 18, No. 2, pp. 667-675